



## Early-age tensile properties of structural epoxy adhesives subjected to low-temperature curing

Omar Moussa, Anastasios P. Vassilopoulos, Julia de Castro, Thomas Keller\*

Composite Construction Laboratory (CCLab), Ecole Polytechnique Fédérale de Lausanne (EPFL), Station 16, Bâtiment BP, CH-1015 Lausanne, Switzerland

### ARTICLE INFO

#### Article history:

Accepted 17 January 2012

Available online 2 February 2012

#### Keywords:

Epoxy/epoxides

Mechanical properties of adhesives

Cure/hardening

Glass transition

### ABSTRACT

The early-age mechanical property development of structural adhesives during low temperature curing is critical for the outdoor construction of engineering structures, such as bridges or buildings. Construction of these structures is also carried out during winter time at low curing temperatures. Experimental investigations showed that the development of the tensile properties of a commercial structural epoxy adhesive strongly depended on the curing temperature. Lower curing temperatures significantly decelerate the process and consequently the rate of development of mechanical properties. At 0 °C, curing was inhibited or did not initiate at all. Tensile strength and stiffness developed at the same rate, although the former was slightly delayed compared to the latter. Significant development of the mechanical properties began only after the onset of material vitrification. This was in contrast to the development of the glass transition temperature, which increased particularly before vitrification. A proposed analytical model predicted the development of mechanical properties well, particularly under low isothermal and cyclic temperature conditions.

© 2012 Elsevier Ltd. All rights reserved.

### 1. Introduction

Adhesive bonding is an advantageous connection technology that is also starting to arouse interest in the construction industry. Up until now, however, adhesives have been mostly used for non-structural or semi-structural connections [1,2], with structural applications being limited to cases where concrete bridge precast segments were bonded together or concrete bridge slabs were bonded to steel girders [3,4]. A recent promising development is the strengthening of structures by bonding fiber-reinforced polymer composite laminates onto existing concrete or steel components [5].

A specific feature of the construction industry is that connections have to be fabricated on site due to time constraints, regardless of the actual environmental conditions and season. Because of this and the generally large scale of the connections, the adhesives used are in most cases cold-curing thermosets. High-temperature curing or post-curing under controlled conditions as in industrial shop fabrication is normally not possible.

In order for adhesive bonding to become widely accepted in the construction industry, bonding during winter time at comparatively low temperatures (5–10 °C) must be possible. The early-stage mechanical properties therefore strongly depend on

the physical state of the adhesive [6]. Curing temperature and curing time govern processes that take place during curing such as gelation and vitrification [7]. As a basis for decisions concerning the duration of construction stages or periods prior to a structure being put into service, there is a need for models allowing prediction of the early-age physical and mechanical properties as a function of (particularly low) curing temperatures and time.

Numerous studies are available that investigate the effects of curing temperature and curing time on the mechanical properties of both bulk adhesive materials and adhesively bonded joints [e.g. 8–11]. However, most of these works focus on hot-curing adhesives and curing temperatures are high compared to those that occur during the winter on a construction site. Furthermore, none of these previous works focused on the relationship between physical properties, such as curing degree or glass transition temperature, and the early-age mechanical properties, particularly under low curing temperatures.

The effects of low temperature curing on the early-age physical properties – curing degree and glass transition temperature – of a commercial structural epoxy adhesive have been investigated by the authors in a previous work [12]. This study focuses on the early-age development of the mechanical properties – tensile stiffness and strength – of the same adhesive subjected to the same low-temperature curing procedures (isothermal, cyclic and outdoor curing). Additionally, the relationship between physical and mechanical properties is established and an

\* Corresponding author. Tel.: +41 21 6933226; fax: +41 21 6936240.  
E-mail address: [thomas.keller@epfl.ch](mailto:thomas.keller@epfl.ch) (T. Keller).

empirical model, based on the autocatalytic curing behavior of the adhesive, is proposed to predict the mechanical properties as a function of the curing procedure.

## 2. Experimental investigation

### 2.1. Adhesive material

The adhesive used was Sikadur-30 from Sika Schweiz AG, a thixotropic bi-component epoxy adhesive, which is typically employed in structural applications and therefore may be seen as representative; a comparison to similar structural adhesives is given in [13]. Components are mixed at a ratio of 3:1 by weight of the respective constituents (resin and hardener). The tensile strength (according to DIN 53 455) and modulus of elasticity (ISO 527) are 31 MPa and 11.2 GPa, respectively; the glass transition temperature of the fully cured material is 62 °C (torsion pendulum according to ASTM D 648) according to the manufacturer. The base resin contains approximately 55% (by weight) silica quartz fillers of sizes ranging between 0.2 and 0.5 mm [12]. The adhesive is used in different applications including structural bonding between FRP composite or steel plates and concrete, different concrete elements and bridge segments.

### 2.2. Curing procedures

Three different curing procedures were applied as follows: (A) Isothermal curing at five different isothermal temperatures ( $T_{cure}=5, 10, 25, 40$  and  $70$  °C) during different curing periods,  $t_{cure}$ , the latter are summarized in Table 1. The temperature range covered the minimum curing temperatures according to the adhesive manufacturer and the maximum temperatures that can occur during summer, e.g. below the asphalt layer of a bridge. The maximum curing time was 720 h (30 days) since only the early age was of interest in this study. (B) Curing at cyclic temperatures between 5 °C and 15 °C and between 0 °C and 10 °C (once starting at 0 °C, and once at 10 °C, see Table 2). The temperatures were kept constant for 12 h and changes then occurred at a rate of approximately 1 °C/min. This curing procedure simulated outdoor situations that can arise during winter time. (C) Complex outdoor curing in winter at varying temperatures from approximately  $-6$  °C to  $+6$  °C for 12 days between 27/01/2010 and 09/02/2010, as shown in Fig. 1.

**Table 1**

Overview of isothermal curing procedure and associated physical (p) and mechanical (m) investigations.

$t_{cure}$ (h)	$T_{cure}$ (°C)				
	5	10	25	40	70
0.17					p
0.33				p	
0.5				p	m
1					p+m
3	p		p		p+m
4		p		p	
6	p		p		p+m
8		p			
16	p		p+m		p+m
24		p+m	p+m		
48	p+m	p+m	p+m		
72	p+m	p+m	p+m		
168	p+m	p+m			
240	p+m	m	m		
720		m			

**Table 2**

Overview of cyclic curing procedure and associated physical (p) and mechanical (m) investigations.

$t_{cure}$ (h)	$T_{cure}$ (°C)		
	0–10	10–0	5–15
24	p		p+m
48	p+m	m	p+m
72	p+m	m	p+m
96			m
120	m	m	
168	m		m

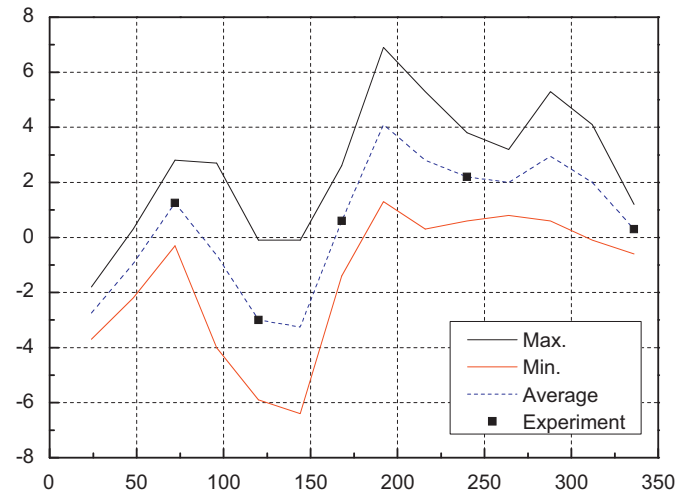


**Fig. 1.** Outdoor curing procedure during winter and associated mechanical investigations.

### 2.3. Investigation of physical properties

A heat-flux differential scanning calorimeter (DSC-TA Q100) connected to a thermal analyzer was used to measure the heat released during the curing reaction. The equipment is supplied by a liquid nitrogen cooling system providing an inert atmosphere, thus allowing the DSC cell to attain low temperature ranges. Samples of 5–10 mg were pre-conditioned in a climate chamber (accuracy of  $\pm 1$  °C) according to curing procedures (A) and (B) during the time periods listed in Tables 1 and 2. Constant humidity ( $50 \pm 2\%$ ) was maintained above 5 °C to eliminate any possible effect on the curing process (below 5 °C humidity could not be controlled). After removal from the climate chamber, the samples were rapidly quenched in liquid nitrogen to stop the curing reaction. Subsequently, the curing degree,  $\alpha$ , (based on the measured residual cure) and the corresponding glass transition temperature,  $T_g$ , of the partially cured samples were obtained by running a dynamic DSC scan. Three samples were investigated for each combination of  $T_{cure}$  and  $t_{cure}$ . Data acquisition was performed using the accompanying software (TA analysis).

### 2.4. Investigation of mechanical properties

Tensile specimens were fabricated in an aluminum mold according to ASTM D638-08 with the dimensions shown in Fig. 2a. The mold was placed in a climate chamber where specimens were cured according to the curing procedures (A) and (B) and time periods listed in Tables 1 and 2. Again, the relative humidity was kept constant at  $50 \pm 2\%$  (above 5 °C). Another set of specimens was subjected to curing procedure (C) according to Fig. 1.

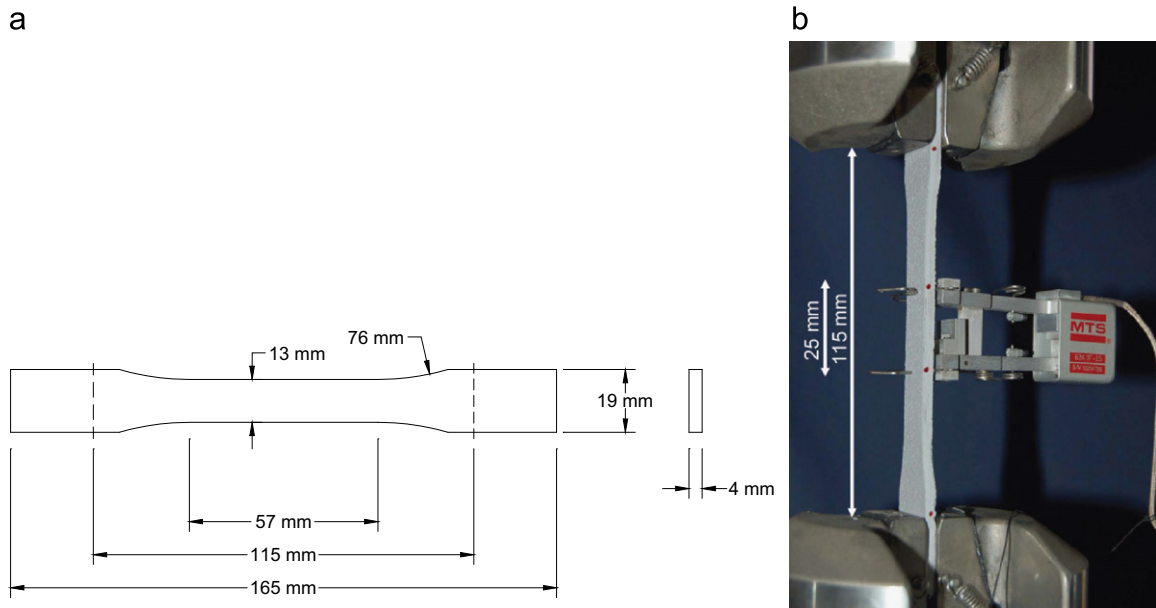


Fig. 2. (a) Specimen dimensions according to ASTM-D638 and (b) experimental setup.

A 10-minute time period was fixed between taking the mold out of the chamber and removing the specimens. One specimen was selected for examination under ambient temperature, while the rest were placed back in the chamber and taken one by one prior to investigation. This was important especially for specimens cured at low temperatures in order to avoid further curing while stored under laboratory conditions. The whole experimental program (physical and mechanical investigation) was performed according to a standard operational procedure (SOP), which had been previously established to ensure the quality and consistency of the results.

Quasi-static tensile experiments were performed according to ASTM D638-08 using an MTS Landmark 25-kN servo-hydraulic load unit calibrated to 20% of its load capacity. Specimens were loaded under displacement control at a loading rate of 5 mm/min. The effect of the loading rate on the resulted strength and stiffness values is not examined in the present work. For determination of Young's modulus,  $E$ , longitudinal strains were measured using an MTS clip-on extensometer, as shown in Fig. 2b. The extensometer had a gage length of  $25 \pm 0.05$  mm and a minimum accuracy of  $\pm 0.5\%$  of the measured strain. A data acquisition system was used to record the time, machine displacement, strain and corresponding load. Five specimens were investigated for each curing combination of  $T_{cure}$  and  $t_{cure}$ . Specimens with voids or other defects in the failure section were not taken into account in the analysis. However, a minimum of three specimens per curing combination was considered in each case.

### 3. Experimental results and discussion

#### 3.1. Physical properties

The development of  $\alpha$  and  $T_g$  at different isothermal temperatures (5, 10, 25 and 70 °C) and cyclic temperatures (0–10 °C and 5–15 °C) are shown in Figs. 3 and 4, respectively. Modeling curves developed in [12] were also added. Curing proceeded and  $T_g$  developed more slowly with decreasing curing temperature. The processes further decelerated after the onset of vitrification, which is indicated by the vitrification curves in Figs. 3 and 4 (defined as points where  $T_g = T_{cure}$ , see [12]). Vitrification,

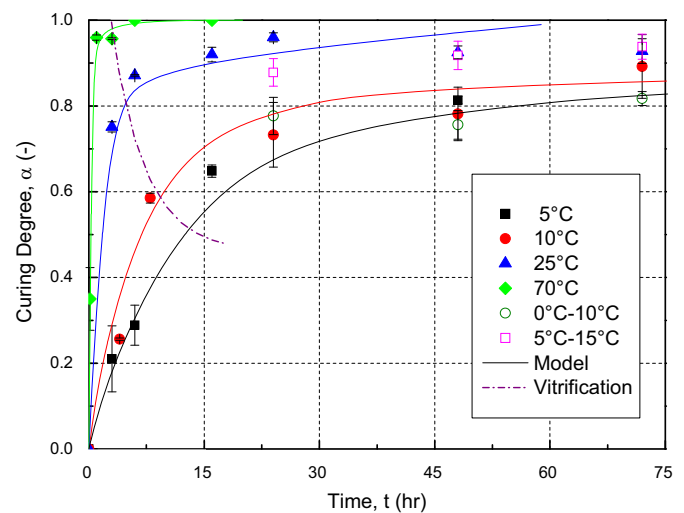


Fig. 3. Curing degree vs. time of partially cured samples at different isothermal and cyclic temperatures.

however, started later when the curing temperature was decreased. The  $T_g$  development at cyclic temperatures (0–10 °C and 5–15 °C) approached that of the corresponding average isothermal temperatures (5 and 10 °C, respectively), as shown in Fig. 4.

The relationship between  $\alpha$  and  $T_g$  for both isothermal and cyclic curing is shown in Fig. 5. A dependence on the curing temperature was observed when curing temperatures were decreased, for both isothermal curing (see [12]) and cyclic curing. This was due to vitrification of the material, which occurred at lower values of  $T_g$  where network density was low [14]. Insufficient activation of the curing reaction greatly decelerated the reaction of secondary amines and sterical hindered amines [14,15].

#### 3.2. Mechanical properties

The development of tensile strength,  $f_t$ , and stiffness (Young's modulus,  $E$ ) vs. time,  $t$ , (up to 2 weeks) during isothermal curing is

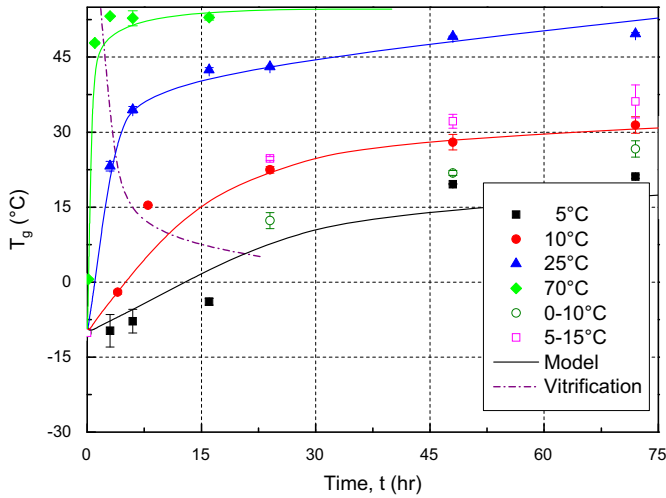


Fig. 4. Glass transition temperature vs. time of partially cured samples at different isothermal and cyclic temperatures.

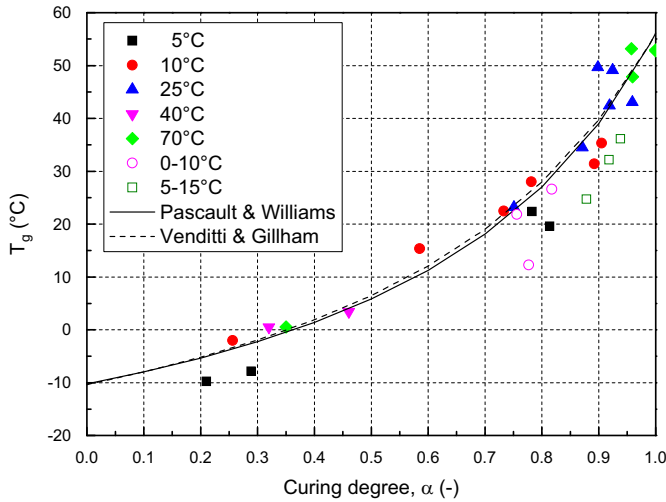


Fig. 5. Glass transition temperature vs. curing degree of partially cured samples at different isothermal and cyclic temperatures.

shown in Fig. 6a and b, respectively. Both properties rapidly increased at high curing temperatures, while a delay in the process was observed particularly during the initial curing stage at low curing temperatures. Fig. 6a and b also shows the curves when vitrification started and significant increases in mechanical properties only occurred after that point, particularly at lower curing temperatures. Since vitrification was delayed at low curing temperatures (see previous section), the development of mechanical properties was also delayed. Furthermore strength, compared to stiffness development, was delayed at low curing temperatures—after 240 h maximum stiffness was reached at all curing temperatures while maximum strength had not yet been reached at the lowest curing temperature of 5 °C. Also, maximum stiffness values were lower at 70 °C curing temperature than those at 25 °C. This was due to the increase in randomness of network crosslinking at high curing temperatures as previously found by Sancaktar et al. [8]. By prolonging the curing period at 10 °C to 720 h (1 month), a slight increase in mechanical properties (around 6% in stiffness and 10% in strength) was achieved compared to those reached after 240 h.

Fig. 7 shows that strength and stiffness relationship was linear, but dependent on curing temperature at later curing stages. The lower the curing temperature, the more strength development

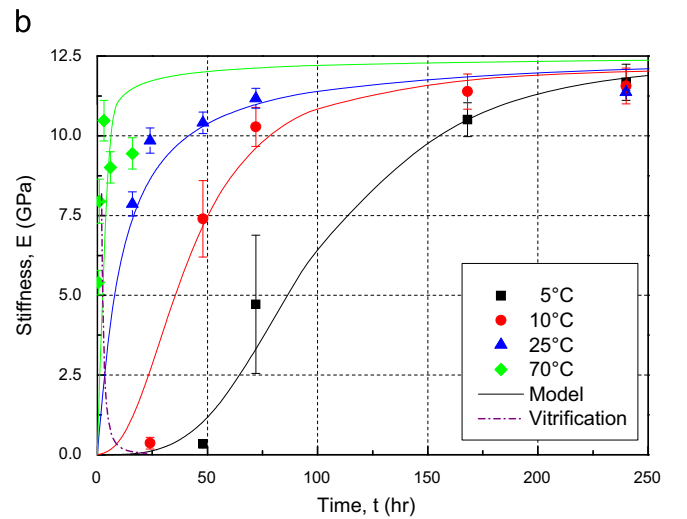
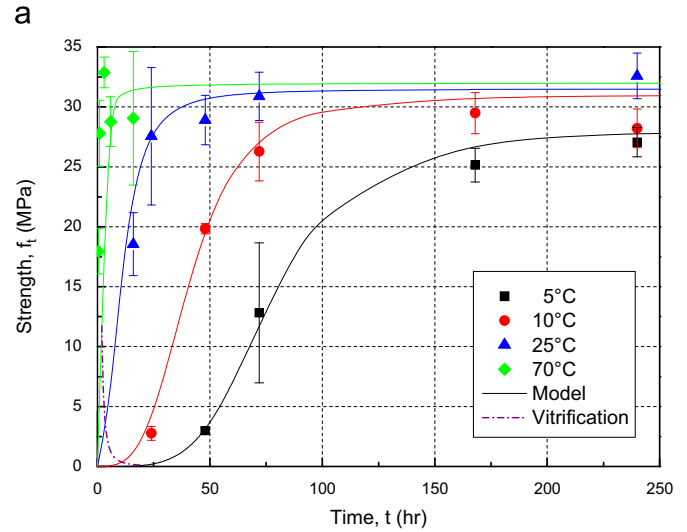


Fig. 6. Mechanical property development at different isothermal temperatures and early stages of curing: (a) strength and (b) stiffness.

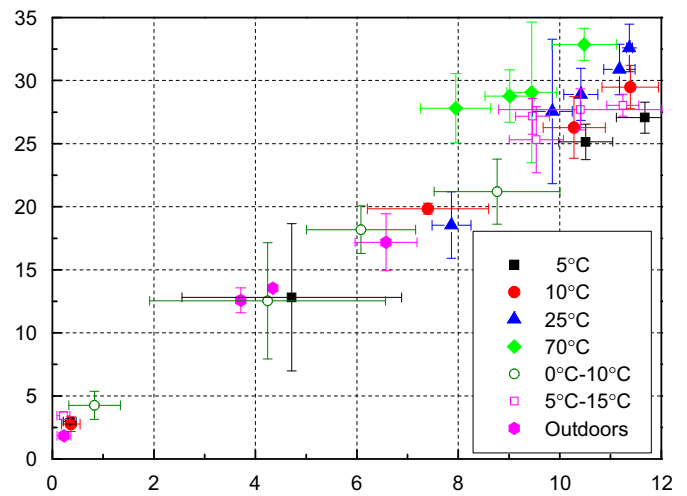


Fig. 7. Strength vs. stiffness relationship.

was delayed compared to stiffness development. The delay in strength development may be attributed to a delay in the development of the molecular bond quality, which depends on curing temperature (see Section 3.3). A potential dependence of

stiffness development on curing temperature may have been masked by the high filler content. The results also show that the scatter in the measured properties tended to be highest when the slope of the curves in Fig. 6 was steepest and then decreased for longer durations.

The tensile strength and stiffness development under cyclic curing are shown in Fig. 8a and b, respectively. The comparison of 0–10 °C and 10–0 °C cycles shows that the former decelerated property development considerably, more than the 12-hour delay introduced at the 10 °C level, and that this difference increased (up to approximately 50 h after 150 h of cure) with further curing. An average increase in mechanical properties of more than 40% was obtained after 72 h when the adhesive curing cycle started by 10 °C instead of 0 °C. Therefore beginning with the 0 °C cycle had a negative effect on the initial crosslinking and continued to have an increasingly negative effect as curing progressed. After around 100 h, however, this was no longer the case since the two curves approached each other. The results also fitted well with the results from isothermal curing shown in Fig. 7. During the 5–15 °C cycles, mechanical properties developed more rapidly as compared to the other two cycles. In addition and similar to the  $T_g$  results (shown in Fig. 4), results of the 5–15 °C cycles and 10 °C isothermal temperature (average temperatures of 5 and 15 °C) agreed well, particularly after 72 h and above.

The outdoor curing results are shown in Fig. 9a and b. Property development started only after 72 h, when the maximum

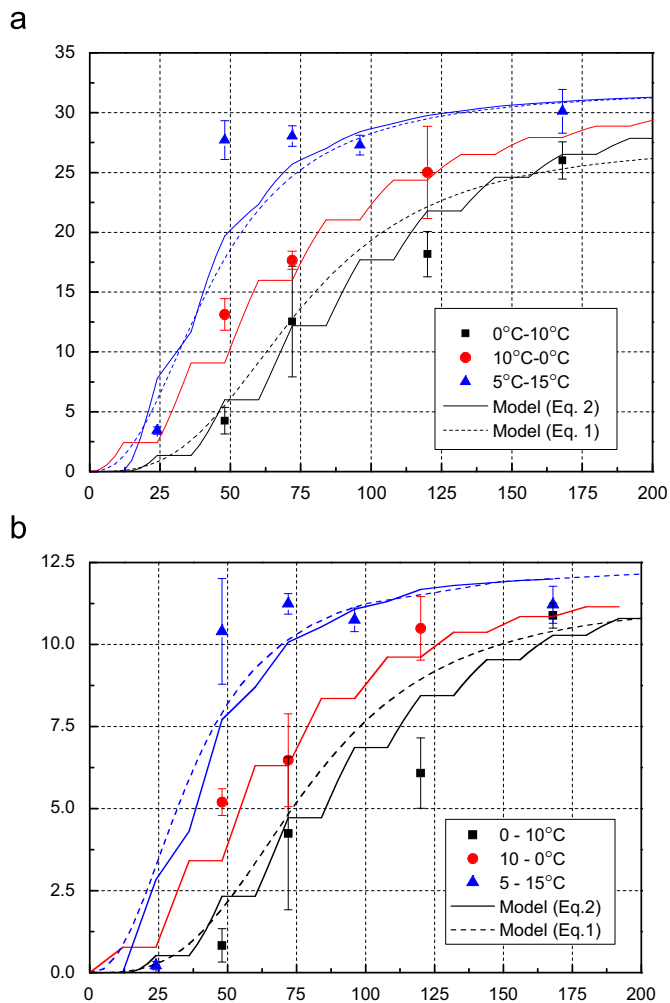


Fig. 8. Mechanical property development at cyclic temperatures and early stages of curing: (a) strength and (b) stiffness.

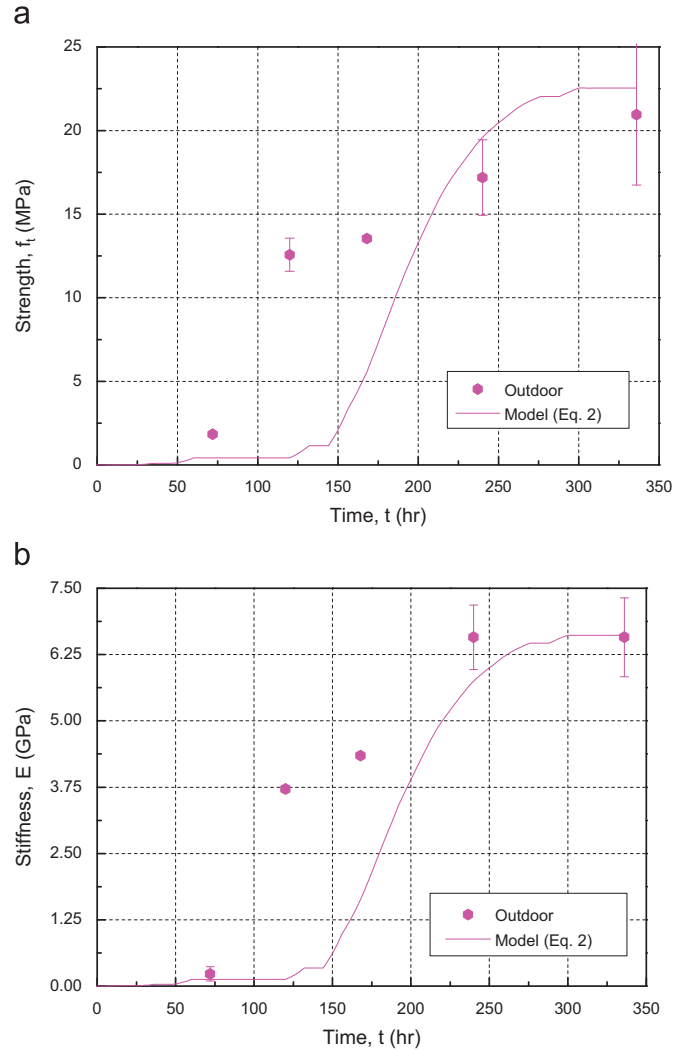
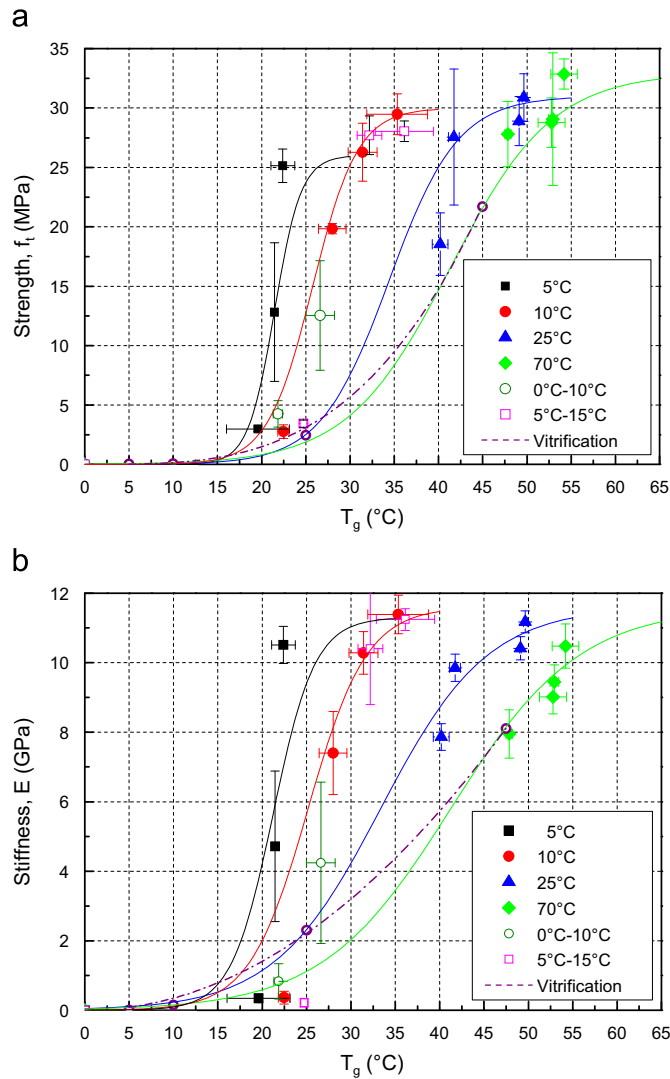


Fig. 9. Mechanical property development during outdoor curing in winter: (a) strength and (b) stiffness.

temperature rose from below 0 °C to almost 3 °C. During the subsequent drop of maximum temperature to 0 °C, the development almost stopped and then restarted when the maximum temperature rose above 0 °C again. When the maximum temperature fell again (but remained around 4 °C), the strength development still continued while stiffness development ceased. As a conclusion of the cyclic and outdoor curing results, 0 °C seems to be the critical temperature at which curing stops or does not start. At slightly higher temperatures (3–5 °C) curing does start, but at a very low rate.

### 3.3. Relationship between physical and mechanical properties

The development of mechanical properties directly depended on changes in the physical state, as shown in Fig. 10, which illustrates the relationship between mechanical properties (strength and stiffness) and physical properties ( $T_g$ ) for the different curing procedures. Fig. 10 also shows the points at which vitrification started. In the first curing phase,  $T_g$  developed significantly in contrast to the mechanical properties, which did not develop at all. The mechanical properties particularly developed after vitrification started, as already discussed in relation to Fig. 6. During this phase,  $T_g$  development dropped behind strength and stiffness development. It seems that the development of the molecular network by crosslinking, expressed by  $T_g$ , and the



**Fig. 10.** Mechanical properties vs.  $T_g$  during different curing procedures: (a) strength and (b) stiffness.

development of the molecular bond quality of the crosslinks did not proceed in parallel. The former process seemed to particularly occur before and the latter particularly after the onset of vitrification. Furthermore – or as an alternative explanation – the decrease in the rate of crosslinking during vitrification of an already strongly crosslinked network was able to over proportionally increase the mechanical properties.

The slope of the curves in Fig. 10 increased with decreasing the curing temperature, i.e. a smaller  $T_g$  increase produced a larger increase of mechanical properties. However, this effect occurred during a much longer time period—it has to be noted that the required curing time is not shown in Fig. 10. Results from cyclic curing fell within same ranges between corresponding isothermal temperatures as in the  $T_g$  vs. time relationship (shown in Fig. 4). Furthermore, Fig. 10 again shows that strength development was behind stiffness development at lower temperatures during the observed early-age period.

#### 4. Modeling and discussion

A model describing the early-age development of mechanical properties as a function of  $T_g$ , as shown in Fig. 6, was established.

A logistic equation according to Gershenfeld [16] was used to describe mechanical behavior since the curing behavior of the epoxy material was autocatalytic (see [12]) and this equation was employed for establishing autocatalytic reaction models. The model takes into consideration the curing temperature-dependent delay at the beginning of property development as well as a plateau at a maximum property value that can be specified. The equation takes the following form:

$$P(t) = \frac{P_0 - P_\infty}{1 + (t/t_m)^s} + P_\infty \quad (1)$$

where  $P(t)$ ,  $P_0$  and  $P_\infty$  are the property values at a given time,  $t$ , at the beginning ( $t=0$ ) and at the end of the curing process, respectively. The parameter  $t_m$  represents the time required to attain a value of  $P_\infty/2$  and  $s$  is the power of the curve (governing the slope of the curve or rate of development). The value  $P_0$  (at the beginning of the curing process) is zero for freshly mixed material while the property end value,  $P_\infty$ , was assumed at 240 h of curing. Accordingly, stiffness was identical for all curing temperatures ( $\sim 11.4$  GPa) while strength at lower curing temperatures was delayed, as previously discussed and shown in Fig. 6a. The relationships of curing temperature,  $T_{cure}$ , vs.  $t_m$ ,  $s$  and  $P_\infty$  (for strength only) are presented in Fig. 11a,b and c, respectively. A similar behavior for both strength and stiffness was obtained from the first two relationships. The time required to attain  $P_\infty/2$  was found to be very similar for strength and stiffness, as shown in Fig. 11a, and the rate of development changed similarly from one curing temperature to another (almost parallel curves). It is obvious from Fig. 11a and b that at temperatures approaching  $0^\circ\text{C}$ ,  $t_m$  and  $s$  tend to infinity, meaning that curing would almost cease at these temperatures, a result that has been confirmed experimentally, as previously shown.

The tensile strength and stiffness at different isothermal temperatures were calculated according to Eq. (1) based on the relationships shown in Fig. 11. A good agreement between experimental and modeling results was found as shown in Fig. 6a and b. In order to predict the results at cyclic temperatures, an extended procedure was used taking the variation of curing temperature and the period during which each temperature was sustained into account. According to this procedure, Eq. (1) can be rewritten as

$$P(t) = \underbrace{\left[ \frac{P_0 - P_{\infty_1}}{1 + (t_1/t_{m_1})^{s_1}} + P_{\infty_1} \right]}_{P_1} + \underbrace{\left[ \frac{P_1 - P_{\infty_2}}{1 + (t_2/t_{m_2})^{s_2}} + P_{\infty_2} \right]}_{P_2} + \dots + \underbrace{\left[ \frac{P_{n-1} - P_{\infty_n}}{1 + (t_n/t_{m_n})^{s_n}} + P_{\infty_n} \right]}_{P_n} \quad (2)$$

with each of the terms of Eq. (2) referring to a single history profile (as a function of curing temperature and curing time) as shown in Figs. 6 and 11. It was assumed that no curing occurred at  $0^\circ\text{C}$ , as mentioned in the above discussion. The modeling results according to Eq. (2), shown in Fig. 8a and b, agree well with the experimental results.

Alternatively, Eq. (1) was applied to also predict mechanical property development under cyclic temperatures by assuming an equivalent curing temperature at the intersection of the  $T_g$  and vitrification curves in Fig. 4 (resulting in a  $T_g$  of  $7.4$  and  $10.1^\circ\text{C}$  for  $0$ – $10$  and  $5$ – $15$  cycles, respectively). The parameters corresponding to the equivalent curing temperatures were again selected from Fig. 11. A good agreement with the experimental results and the results of Eq. (2) was obtained, see Fig. 8 (model Eq. (1)).

The model Eq. (2) was also applied to predict the behavior of outdoor specimens during early-age curing; Fig. 9 shows the strength and stiffness results. The development after around 150 h was well predicted, while the effect of the first low temperature peak between approximately 50 and 100 h, see Fig. 1, was underestimated. Although the maximum temperature during this period was below  $3^\circ\text{C}$ , this

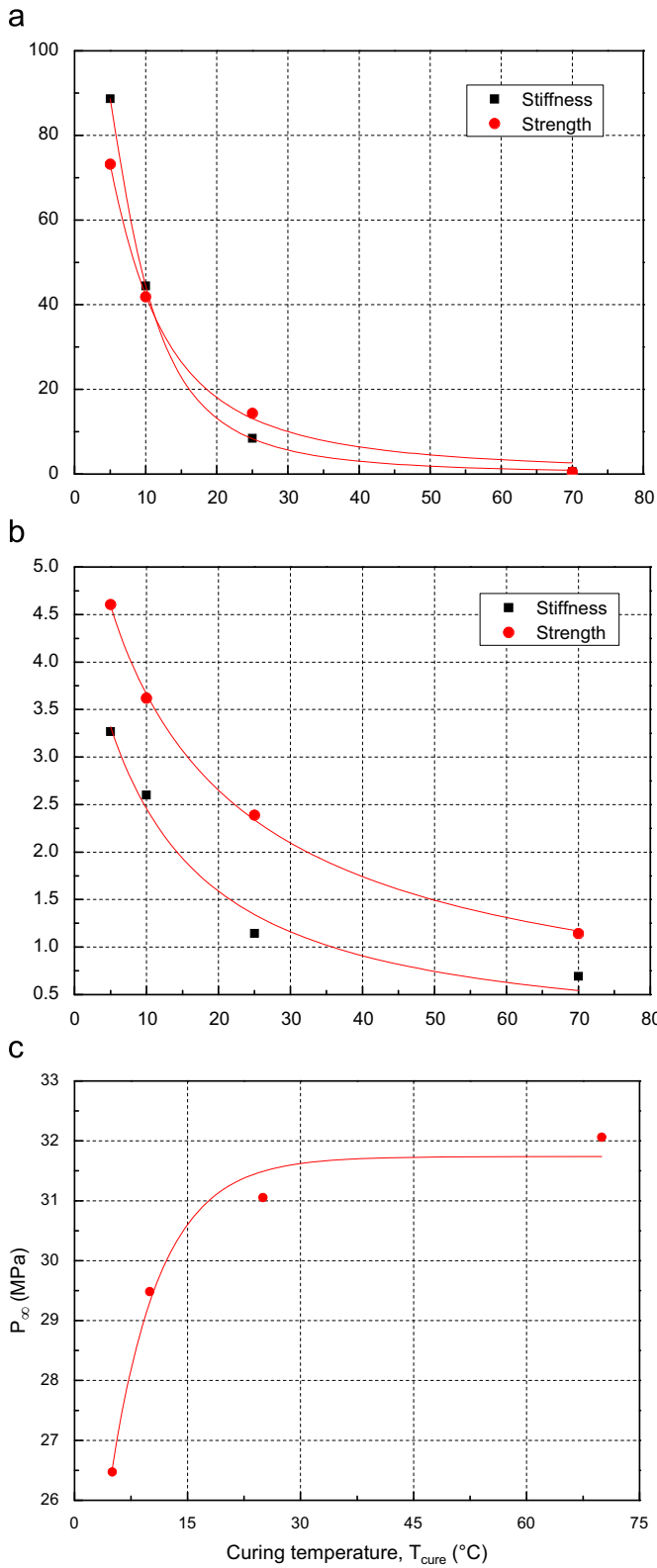


Fig. 11. Model parameters as a function of curing temperature: (a)  $t_m$ ; (b)  $s$  and (c)  $P_{\infty}$ .

level already produced a significant increase of the mechanical properties. It should be noted that the available data only comprised the highest and lowest temperatures of a given day, excluding details concerning the change of temperature during the same day. Furthermore, other potential effects, such as humidity, were unknown. This may also explain the deviations of the predictions.

## 5. Consequences for outdoor construction

As already mentioned, civil engineering structures – in particular bridges where adhesive connections can offer significant advantages – are built throughout the year and construction cannot be interrupted during winter time. The results of this study demonstrate that adhesive bonding in winter, at low temperatures, is possible. Curing and the associated physical and mechanical properties already develop at temperatures slightly above 0 °C. Curing is very slow, however, and one of the main advantages of adhesive bonding in bridge construction – the fast execution of load-bearing joints – is lost, unless the joint is artificially heated during fabrication. The latter may offer a valuable solution for steel joints where the adherends have high thermal conductivity. In concrete construction, however, this is much more difficult.

On the other hand, bridge construction, in most cases, occurs in different stages and during the construction stages full mechanical properties are often not required. The models developed above allow the required curing time to be estimated as a function of curing temperature and, based on the required level of full mechanical properties, can serve as a useful tool for establishing the time schedule for construction stages. Fig. 12, for instance, shows the tensile strength and stiffness of the adhesive used in

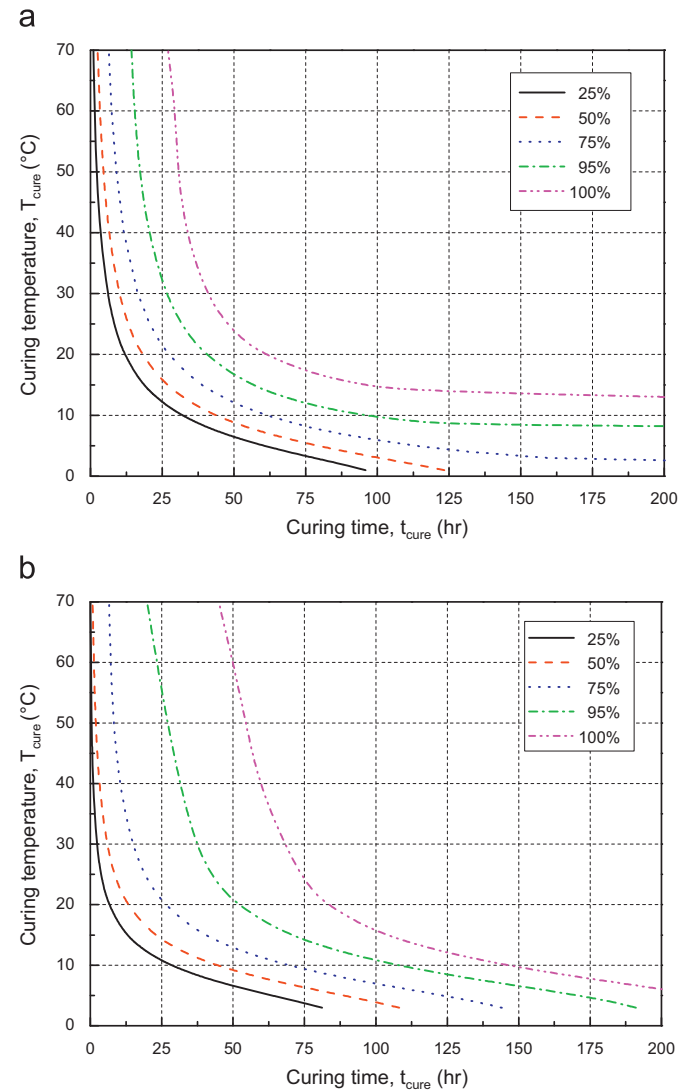


Fig. 12. Mechanical property levels as a function of curing conditions: (a) strength and (b) stiffness.

this study as a function of curing temperature and curing time (as a percentage of maximum (100%)) properties at 240 h according to Fig. 6. The curves were derived from the model developed above.

## 6. Conclusions

Experimental and analytical investigations concerning the early-age development of mechanical tensile properties of a structural epoxy adhesive were performed. The effects of different curing procedures and the associated physical material states on the mechanical properties were investigated. The following conclusions can be drawn:

- (1) The mechanical properties started developing significantly only after the onset of material vitrification. This was in contrast to the development of the glass transition temperature, which particularly increased before vitrification and leveled off during vitrification.
- (2) The mechanical property development strongly depended on the curing temperature. Lower curing temperatures significantly decelerated the process. At 0 °C curing was inhibited or did not start at all.
- (3) Strength and stiffness developed at the same rate. Strength development, however, was slightly delayed at later stages of cure compared to stiffness development at low curing temperatures.
- (4) An analytical model is proposed that can predict the development of mechanical properties under isothermal and cyclic curing conditions. Modeling and experimental results compared well.
- (5) Based on the analytical model, design curves for early-age mechanical properties as a function of curing temperature and time can be established.

## Acknowledgments

The authors thank the Federal Roads Authority (FEDRO) for funding this project, SIKA AG, Zurich, for its support, and the

Laboratory of Composite and Polymer Technology (LTC—EPFL) for use of DSC equipment.

## References

- [1] Dunn DJ. Engineering and structural adhesives. *Rapra Rev Rep* 2004;15(1): 1–28.
- [2] Mays GC, Hutchinson AR. Adhesives in civil engineering. Cambridge University Press; 1992.
- [3] Fiedler E. Die Entwicklung des Stahlbrückenbaues in der DDR bis zum Zeitpunkt der Wende ein Rückblick (Teil II). *Stahlbau* 2001;70(5):317–28.
- [4] Buyukozturk O, Bakhoum MM, Beattie SM. Shear behavior of joints in precast concrete segmental bridges. *J Struct Eng* 1990;116(12):3380–401.
- [5] Meier U. Strengthening of structures using carbon fibre/epoxy composites. *Contr Build Mater* 1995;9(6):341–51.
- [6] Jordan C, Galy J, Pascault JP. Measurement of the extent of reaction of an epoxy-cycloaliphatic amine system and influence of the extent of reaction on its dynamic and static mechanical properties. *J Appl Polym Sci* 1992; 46(11–12):859–71.
- [7] Wisanrakkit G, Gillham JK. Glass transition temperature ( $T_g$ ) as an index of chemical conversion for high- $T_g$  amine/epoxy system: chemical and diffusion-controlled reaction kinetics. *J Appl Polym Sci* 1990;41(5):2885–929.
- [8] Sancaktar E, Hooshang J, Klein RM. The effects of cure temperature and time on the bulk tensile properties of a structural adhesive. *J Adhes* 1983; 15(3–4):241–64.
- [9] Shaw SJ, Tod DA. The effect of cure conditions on a rubber-modified epoxy adhesive. *J Adhes* 1989;28(4):231–46.
- [10] Sinclair JW. Effect of cure temperature on epoxy resin properties. *J Adhes* 1992;38:219–34.
- [11] Lapique F, Redford K. Curing effects on viscosity and mechanical properties of commercial epoxy resin adhesive. *Int J Adhes Adhes* 2002;22(4):337–46.
- [12] Moussa O, Vassilopoulos A, Keller T. Effects of low temperature curing on physical properties of structural epoxy adhesive joints in bridge construction. *Int J Adhes Adhes* 2012;32(1):15–22.
- [13] Moussa O, Vassilopoulos A, Keller T. Experimental DSC-based method to determine glass transition temperature during curing of structural adhesives. *Constr Build Mater* 2012;28(1):263–8.
- [14] Ehrenstein GW, Pongratz S. Beständigkeit von Kunststoffen. München: Carl Hanser Verlag; 2007.
- [15] Bauer RS. Epoxy Resins, ACS Symposium Series 285, Applied Polymers Science. 2nd ed. Washington: ACS; 1985.
- [16] Gershenfeld NA. The nature of mathematical modeling. Cambridge University Press; 1999.